

Study on the characteristics of an imaging spectrum system by means of an acousto-optic tunable filter

Yan Cui*
Dunjie Cui
Jiuhua Tang
Academia Sinica
Changchun Institute of Optics and Fine
Mechanics
P.O. Box 1024
Changchun, 130022, China

Abstract. The spectrally agile staring sensor (SASS) is an instrument system that is able to acquire image and spectrum information simultaneously. We analyze the expression of SNR and overall performance of the SASS system consisting of an acousto-optic tunable filter and point out improvement methods and limiting factors of the system performance. The complete SASS system setup is constructed. By means of this setup, the theoretical analysis is verified and the image and spectrum information of the simulated target is obtained. These results demonstrate the ability of the SASS to acquire image and spectrum information.

Subject terms: imaging; spectrums; acousto-optics; filters.
Optical Engineering 32(11), 2899–2903 (November 1993).

1 Introduction

The purpose of imaging spectroscopy is to acquire image and spectrum information simultaneously. One of the instrument systems that can achieve this aim is the spectrally agile staring sensor (SASS). This concept was first introduced by Kollodge et al.¹ in 1981. The schematic diagram of SASS is shown in Fig. 1. The light from a target is focused on a 2-D array of detectors by the optics, and a spectral filter is placed immediately in front of the detectors. A series of monochromatic images of the target can be acquired by tuning the passband of the spectral filter. SASS has advantages such as simple construction, high optic efficiency, etc. These advantages give it potential for use in remote sensing.

Kollodge et al.¹ and Babrov and Jacobs² have given the design results for when the target behaves as a classical point

source. No research has been reported about the situation where the target behaves as an area source, which is the most common case in remote sensing. In this paper, we treat the target as an area source and choose an acousto-optic tunable filter (AOTF) as the spectral filter of the SASS system. The SNR and overall performance analysis of the SASS system consisting of an AOTF is given in Sec. 2. Next, the complete SASS system setup we constructed is reported. By means of this setup, the theoretical analysis is verified and the image and spectrum information of a simulated target is acquired.

2 Performance Analysis of the SASS System

The spectral filter is one of the key parts of SASS; its type, construction, and characteristics determine the system design and performance. The AOTF is one of the prospective spectral filters that can be used in the SASS system. It is an electronically tuned optic filter that operates on the principle of acousto-optic diffraction in an optically anisotropic medium.³ The acoustic wave propagating in the acousto-optic medium modulates the index of refraction of the medium periodically, so the medium disperses light just as a phase grating. The spectral transmission of an AOTF for incident

*Current affiliation: Academia Sinica, State Key Laboratory of Transient Optics Technology, Xi'an Institute of Optics and Precision Mechanics, P.O. Box 80, Xi'an, 710068, China.

Paper 26072 submitted by Acta Optica Sinica; received Aug. 1, 1992; revised manuscript received Feb. 1, 1993; accepted for publication Feb. 1, 1993.
© 1993 Society of Photo-Optical Instrumentation Engineers. 0091-3286/93/\$6.00.

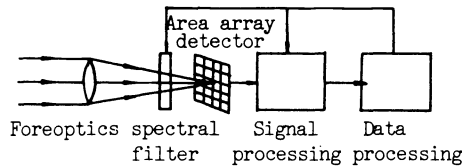


Fig. 1 Schematic diagram of SASS.

parallel light has been derived by Harris and Wallace,⁴ and is expressed as $h(\lambda, \lambda_0, \alpha, \beta, r)$, where λ_0 is the central wavelength of the AOTF passband; α and β are the polar and azimuthal angles, respectively, of the deviation of incident light from incident angles determined by momentum match conditions; and r is the ratio of real acoustic power to that needed for 100% diffraction efficiency. Also, $h(\lambda, \lambda_0, \alpha, \beta, r)$ is a function of the AOTF construction parameters. When the wavelength λ deviates from λ_0 , or α and β deviate from zero values, the value of $h(\lambda, \lambda_0, \alpha, \beta, r)$ decreases. When $h(\lambda, \lambda_0, \alpha, \beta, r)$ reaches its first minimum, the corresponding deviation of λ is defined as the passband width (denoted by $\Delta\lambda_0$), and the corresponding deviations of α and β are defined as polar and azimuthal aperture angles (denoted by α_0 and β_0), respectively. Here, $\Delta\lambda_0$, α_0 , and β_0 are somewhat different from those defined by Ref. 3 for the convenience of normalized analysis of the AOTF transmission.

When an AOTF is used in a SASS system, the incident light beam is a cone. Assume the intensity distribution of an incident cone of light is uniform. Then, the spectral transmission of the AOTF for the incident cone of light is

$$T(\lambda, \lambda_0, \Omega, r) = \iint h(\lambda, \lambda_0, \alpha, \beta, r) d\alpha d\beta / \Omega, \quad (1)$$

where Ω is the solid angle of the cone of light, and the limits of integration are set by the cone of light. The light at different wavelengths that is diffracted by the AOTF all reaches the focal plane of the system, so the quantity corresponding to the signal level is $\int T(\lambda, \lambda_0, \Omega, r) d\lambda$. As the expression of $h(\lambda, \lambda_0, \alpha, \beta, r)$ is sophisticated, it is impossible to integrate $T(\lambda, \lambda_0, \Omega, r)$ over λ analytically. To get an analytical expression for system design guidance, the AOTF performance parameters $\Delta\lambda_0$, α_0 , and β_0 are used to replace the construction parameters in $h(\lambda, \lambda_0, \alpha, \beta, r)$. The function $h(\lambda, \lambda_0, \alpha, \beta, r)$ is simplified further by means of the normalized parameters $(\lambda - \lambda_0) / \Delta\lambda_0$, α / α_0 , and β / β_0 . The final result obtained by numerical integration is⁵

$$\int T(\lambda, \lambda_0, \Omega, r) d\lambda = \Delta\lambda_0 D(r), \quad (2a)$$

$$\Delta\lambda = F(\Omega / \alpha_0 \beta_0) \Delta\lambda_0, \quad (2b)$$

where $D(r)$ is the factor that is relevant to the acoustic power in the acousto-optic medium whose curve obtained by numerical integration is shown in Fig. 2, $\Delta\lambda$ is the passband width of the AOTF for the incident cone of light, and $F(\Omega / \alpha_0 \beta_0)$ is the passband widening factor (i.e., $\Delta\lambda / \Delta\lambda_0$) obtained by numerical integration whose curve is shown in Fig. 3. In fact, $D(r)$ is the integration of the AOTF transmittance over the normalized parameter $(\lambda - \lambda_0) / \Delta\lambda_0$. It arises from the variation of diffraction efficiency with acous-

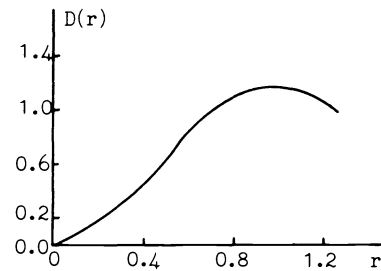


Fig. 2 Function $D(r)$ by numerical integration.

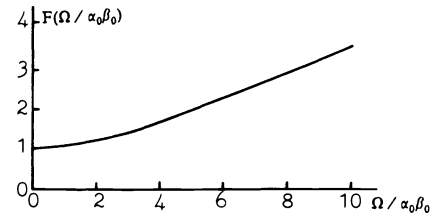


Fig. 3 Function $F(\Omega / \alpha_0 \beta_0)$ by numerical integration.

tic power and reaches its maximum when $r=1$; $F(\Omega / \alpha_0 \beta_0)$ arises from the variation of the diffraction wavelength with the incident angle, and the numerical integration results show that $F(\Omega / \alpha_0 \beta_0)$ is hardly relevant to parameter r , therefore, the parameter r is isolated from the solid angle Ω in Eq. (2b). From the physical point of view, the transmission of AOTF for the incident cone of light is the convolution of that for the incident parallel of light over the solid angle, so $\Delta\lambda$ should equal the square root of the sum of $\Delta\lambda_0$ squared and the solid angle contribution squared, i.e., $F(\Omega / \alpha_0 \beta_0)$ should have the form $[1 + k(\Omega / \alpha_0 \beta_0)^2]^{1/2}$, where k is a factor that expresses the extent of the solid angle contribution. Thus, $F(\Omega / \alpha_0 \beta_0)$ becomes a linear function approximately when $\Omega / \alpha_0 \beta_0 \gg 1$. Because the preceding analysis is based on the normalized method, the result does not vary with the AOTF construction parameters; it is universal.

When the target behaves as an area source, the relevant radiometric quantity to describe the source is the spectral radiance N_λ (in units of $\text{W nm}^{-1} \text{cm}^{-2} \text{Sr}^{-1}$). The SNR analysis discussed here is based on the SASS system with detectors that are in direct contact with a mosaic of CCDs, so the performance of the detectors can be described by the spectral noise equivalent exposure NEE_λ (in units of J cm^{-2}). Assume the spectral radiance of the target N_λ , the spectral transmittance of the atmosphere $\tau_{a,\lambda}$, and the optics $\tau_{o,\lambda}$ change slightly within the passband of AOTF. Then, the SNR expression of the SASS system can be written as follows:

$$(S/N)_{\lambda_0} = (N_{\lambda_0} \tau_{a,\lambda_0}) (\tau_{o,\lambda_0} \Omega) (t_i / NEE_{\lambda_0}) \int T(\lambda, \lambda_0, \Omega, r) d\lambda, \quad (3)$$

where t_i is the integrating time of the CCD. Equation (3) shows that the SNR of the SASS system is determined by the mission condition $N_{\lambda_0} \tau_{a,\lambda_0}$, optics $\tau_{o,\lambda_0} \Omega$, detectors t_i / NEE_{λ_0} , and spectral filter $[\int T(\lambda, \lambda_0, \Omega, r) d\lambda]$. Using Eqs. (2a) and 2(b), Eq. (3) can be rewritten as follows:

$$\left(\frac{S}{N}\right)_{\lambda_0} \left(\frac{1}{\Delta\lambda}\right) \left(\frac{1}{t_i}\right) = \frac{(N_{\lambda_0} \tau_{a,\lambda_0})(\tau_{o,\lambda_0} \Omega) D(r)}{F(\Omega/\alpha_0 \beta_0) NEE_{\lambda_0}} \quad (4)$$

The parameters on the left side of Eq. (4) represent the signal resolution S/N , wavelength resolution $1/\Delta\lambda$, and information recording rate $1/t_i$, respectively. Multiplication of these parameters represents the power of the system to obtain information and evaluates the overall performance of the system.⁶ The right side of Eq. (4) is related to the mission condition, optics, filter, and detectors. When these have been determined, the three performance parameters on the left side of Eq. (4) restrain each other; the enhancement of one performance parameter must be at the expense of others. Therefore, the way to enhance the overall performance of the system is to choose the parameters on the right side of Eq. (4) and maximize them. The corresponding methods are as follows:

1. enhance the transmittance of optics by design or coating,
2. choose the 2-D array of detectors that have small NEE_{λ} ,
3. choose the AOTF that has high diffraction efficiency (r is near 1),
4. enlarge the aperture of the optics (i.e., Ω) [However, when $\Omega/\alpha_0 \beta_0 > 4$, and $\Omega/F(\Omega/\alpha_0 \beta_0)$ is near constant, it is of no use to enlarge Ω further.]
5. choose the AOTF that has large aperture angles, which makes $F(\Omega/\alpha_0 \beta_0)$ smaller at the same Ω .

Of course, these methods may be limited by materials, design, and fabrication technology, so the overall performance of the system can be enhanced only in an allowed range.

3 Experiments

The experimental setup of the complete SASS system constructed by us is shown in Fig. 4, and its schematic diagram is shown in Fig. 5. The tuning range of the AOTF used in the setup is 500 to 680 nm, the passband width of the AOTF at the 580-nm wavelength is 3.5 nm for a parallel beam of light, the pixel number of the Si-CCD used in the setup is

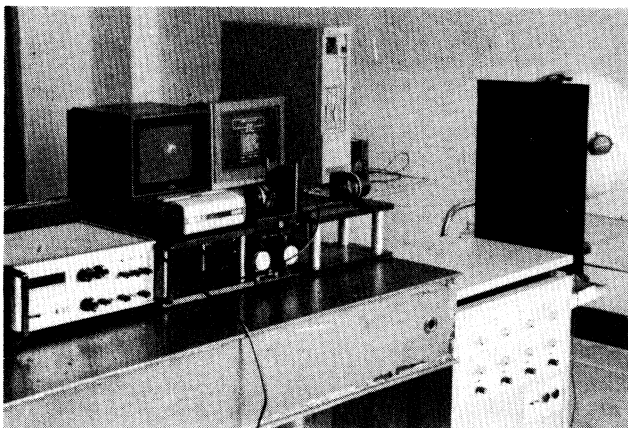


Fig. 4 Experimental setup of the complete SASS system.

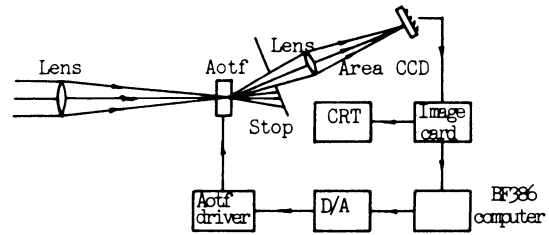


Fig. 5 Schematic diagram of the SASS experimental setup.

500(H) \times 582(V), the pixel dimension is 17 μm (H) \times 13 μm (V), the dynamic range is 100:1, NEE_{λ} is about 0.1 nJ cm^{-2} , and the integrating time is 40 ms. The performance measurement results of the setup show that the image resolution is 4.2 lp/mrad, which is mainly limited by CCD pixel distance; the passband width at 580 nm is 3.8 nm, which is determined by the AOTF passband width and the solid angle of the incident cone of light; and the dynamic range of the setup is 50:1, which is due to the small dynamic range of the Si-CCD and the stray light introduced by interface reflection.

3.1 Verification of Theoretical Analysis

By means of the experimental setup constructed by us, the SNR expression obtained by theoretical analysis is verified. The diffraction efficiency of the AOTF varies with the light incident position because of the attenuation of acoustic wave propagating. The diffraction efficiency of the AOTF at four distances along the path of acoustic propagation was measured in the experiment and found to be 80, 79, 64, and 42% at the 580-nm wavelength. The source is a white plate irradiated by a standard lamp and its spectral radiance at the 580-nm wavelength is 2.94 $\mu\text{W}/(\text{nm cm}^2 \text{ Sr})$, where $\Omega = 0.02124 \text{ Sr}$, $\tau_{o,\lambda} = 0.45$, and $\tau_{a,\lambda} = 1$. By means of these quantities and Eq. (4), the SNR values for the four distances are calculated; they are listed in Table 1. The measured SNR values are also listed in Table 1 and are obtained by 31 repeated measurements of the monochromatic image at the 580-nm channel. The relative error between the theoretical calculation and the experiment is in the range of 7 to 17%. One of the reasons for this error is the diffraction efficiency measurement error, which is about 4%. But the main reason is the noise measurement error; because of the randomness of noise, its measurement nonrepeatability in our experiment is as high as 20%. In addition, the parameter NEE_{λ} used in the theoretical calculation, which is given by device instruction, may vary with different devices.

Equations (2a) and (2b) are also verified by experiment. The central wavelength of the test channel is 580 nm. With $\Omega/\alpha_0 \beta_0$ varying from 0 to 2.5, the relative error between the theoretical calculations and the experimental results is 5%.

Table 1 Comparison between calculated and measured SNR.

Diffraction efficiency	80%	79%	64%	42%
Calculated SNR	31.3	30.7	25.0	15.1
Measured SNR	37.5	36.6	27.6	14.1

3.2 Acquisition of Image and Spectrum Information

To demonstrate the ability of the SASS experimental setup to obtain image and spectrum information, a red filter placed on the open hole of an integrating sphere is used as a source. The filter transmission measured by the SASS experimental setup is shown in Fig. 6(a). The measurement results from a Shimadzu UV 210 spectrophotometer are shown in Fig. 6(b) for comparison. It can be seen from Fig. 6 that the wavelength calibration of the SASS experimental setup is accurate; the difference is that the curve in Fig. 6(a) is about 5% higher than the curve in Fig. 6(b) in the shorter wavelength range, which is due to the stray light introduced by interface reflection. Another difference is that the curve measured by the SASS experimental setup fluctuates because of the low SNR of the system.

A slide is used to replace the red filter as a simulated target. It consisted of a red flower with a yellow center and a number of light green leaves. Figure 7 shows a series of monochromatic images of the simulated target obtained from the SASS experimental setup. The wavelength changes from 555 to 665 nm in steps of 10 nm. It can be seen from Fig. 7 that the leaves are brighter than the flower at shorter wavelengths. As the wavelength becomes longer, the leaves become dimmer, and the flower becomes brighter. The center of the flower maintains brightness at all wavelengths. Once the image data at different wavelengths have been recorded, the spectrum information of each pixel can be extracted easily by computer.

4 Conclusions

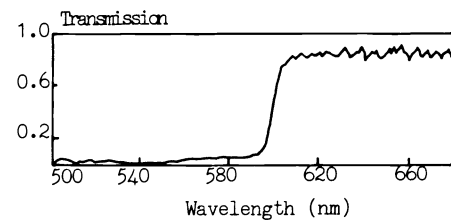
The expressions of SNR and overall performance of the SASS system have been given by theoretical analysis. The methods to enhance the system performance have been discussed. These results provide guidance for the SASS system design. The experimental setup of the complete SASS system has been constructed. By means of this setup, the theoretical analysis has been verified and accordance error is about 10%. The experiments show that the SASS system consisting of an AOTF is able to obtain both image and spectrum information of the target. The disadvantages of the current setup include small dynamic range and narrow spectral tuning range. If the AOTF used in the setup is coated with antireflection film and some stops are set in the setup, the stray light in the SASS system will be decreased by one order of magnitude and the dynamic range of the system will be increased to 60:1. Furthermore, if a 2-D array of detectors whose dynamic range is 500:1 is used in the SASS system, the dynamic range of the system will be increased to about 300:1. The tuning range of the setup is limited by the AOTF at present. The narrow tuning range of the AOTF is due to impedance mismatching between the AOTF and its driver, and it can be widened to one octave by the matching circuit.

Acknowledgment

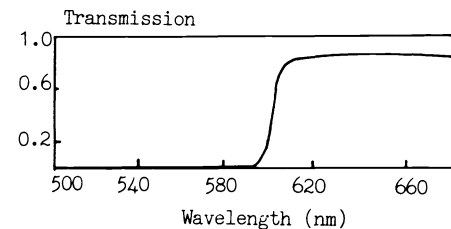
The authors wish to thank Prof. Li Juenjie for his support of the fabrication of the AOTF.

References

1. M. A. Kollodge, J. A. Cox, W. C. Marshall, R. G. Solstad, and S. S. Steadman, "Design studies for a spectrally agile staring sensor (SASS) system," *Proc. SPIE* **265**, 140–155 (1981).



(a)



(b)

Fig. 6 Filter transmission measured by (a) the SASS experimental setup and (b) a spectrophotometer.

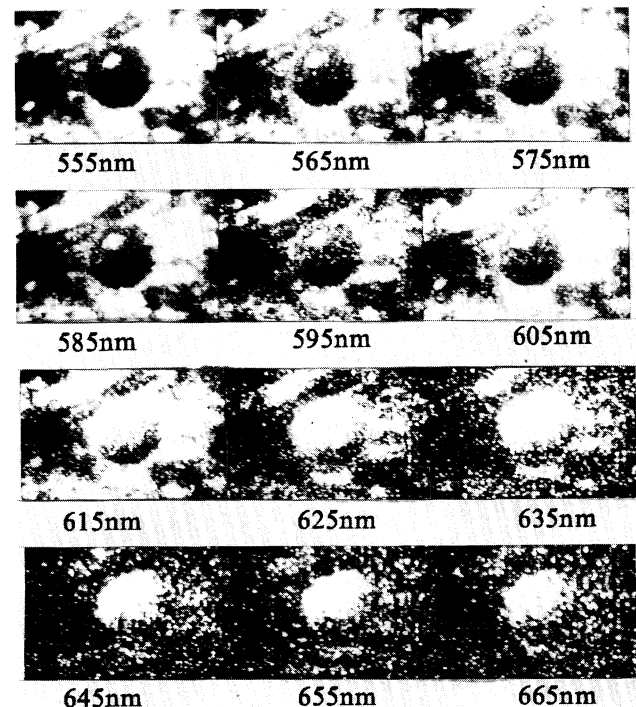
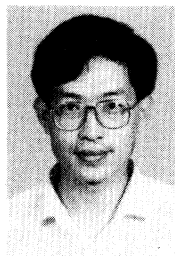


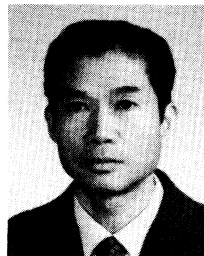
Fig. 7 Monochromatic images of the simulated target measured by the SASS experimental setup.

2. H. J. Babrov and M. M. Jacobs, "Acousto-optic tunable filter performance in a staring IR sensor," *Appl. Opt.* **18**(23), 3901–3907 (1979).
3. I. C. Chang, "Acousto-optic tunable filter," *Opt. Eng.* **20**(6), 824–829 (1981).
4. S. E. Harris and R. W. Wallace, "Acousto-optic tunable filter," *J. Opt. Soc. Am.* **59**(6), 744–747 (1969).
5. Y. Cui and M. Zhang, "Acousto-optic tunable filter transmission characteristic analysis for incident cone of light," *Proc. SPIE* **1814**, 160–166 (1992).
6. J. Tang, "On problems towards the promotion of instrument layout design," *Acta Optica Sinica* **1**(1), 67–74 (1981).

CHARACTERISTICS OF AN IMAGING SPECTRUM SYSTEM



Yan Cui received his BS and MS degrees from the Changchun College of Optics and Fine Mechanics and his PhD degree from the Changchun Institute of Optics and Fine Mechanics, Academia Sinica, all in optics, in 1984, 1987, and 1991, respectively. He works as a post doctor at the State Key Laboratory of Transient Optics Technology, Xi'an Institute of Optics and Precision Mechanics. His research interest is spectral radiation measurement.



Jiu Hua Tang received his BS degree from Shanghai Jiaotong University in 1951. He is now a professor at the Changchun Institute of Optics and Fine Mechanics, Academia Sinica. He was elected as a member of the Chinese Academy of Sciences in 1991. His research interests include mechanics and instrument layout design.



Dunjie Cui received his BS degree in physics from Jilin University in 1962. He then joined the Changchun Institute of Optics and Fine Mechanics, Academia Sinica, as an associate professor. His research interests include methods and instruments of radiation measurement.